REPORTS OF PRACTICAL
ONCOLOGY AND
RADIOTHERAPY

Optimized target delineation procedure for the radiosurgery treatment of ventricular tachycardia: observer-independent accuracy

Authors: Jan Hecko, Lukas Knybel, Marian Rybar, Marek Penhaker, Otakar Jiravský, Radek Neuwirth, Marek Sramko, Jana Haskova, Josef Kautzner, Jakub Cvek

Optimized target delineation procedure for the radiosurgery treatment of ventricular tachycardia: observer-independent accuracy

Running head Optimized target delineation for STAR

Jan Hecko[1, 2], Lukas Knybel[3, 4], Marian Rybar[5], Marek Penhaker[2], Otakar Jiravsky[1, 6], Radek Neuwirth[1, 6], Marek Sramko[7], Jana Haskova[7], Josef Kautzner[7], Jakub Cvek[3, 4]

[1]Department of Cardiology, Podlesi Hospital, Trinec, Czech Republic

[2]VŠB-Technical University of Ostrava, Ostrava, Czech Republic

[3]Department of Oncology, University Hospital Ostrava and, Ostrava, Czech Republic

[4]Faculty of Medicine, University of Ostrava, Ostrava, Czech Republic

[5]Department of Biomedical Technology ,Czech Technical University in Prague,Kladno, Czech Republic

[6]Faculty of Medicine, Masaryk University, Brno, Czechia

[7]Institute for Clinical and Experimental Medicine, Prague, Czech Republic

Corresponding Author: Lukas Knybel, Department of Oncology, University Hospital Ostrava and, Ostrava, Czech Republic; e-mail: lukas.knybel@fno.cz

Abstract

Background: Part of the current stereotactic arrythmia radioablation (STAR) workflow is transfer of findings from the electroanatomic mapping (EAM) to computed tomography (CT).

Here, we analyzed inter- and intraobserver variation in a modified EAM-CT registration using automatic registration algorithms designed to yield higher robustness.

1

Materials and methods: This work is based on data of 10 patients who had previously undergone STAR.

Two observers participated in this study: (1) an electrophysiologist technician (cardiology) with substatial experience in EAM-CT merge, and (2) a clinical engineer (radiotherapy) with minimum experience with EAM-CT merge.

EAM-CT merge consists of 3 main steps: segmentation of left ventricle from CT (CT LV), registration of the CT LV and EAM, clinical target volume (CTV) delineation from EAM specific points.

Mean Hausdorff distance (MHD), Dice Similarity Coefficient (DSC) and absolute difference in Center of Gravity (CoG) were used to assess intra/interobserver variability.

Results:

Intraobserver variability: The mean DSC and MHD for 3 CT LVs altogether was 0.92 ± 0.01 and 1,49 ± 0,23 mm. The mean DSC and MHD for 3 CTVs altogether was 0,82 ± 0,06 and 0,71 ± 0,22 mm.

Interobserver variability: Segmented CT LVs showed great similarity (mean DSC of 0,91 ± 0,01, MHD of 1,86 ± 0,47 mm). The mean DSC comparing CTVs from both observers was 0,81 ± 0,11 and MHD was 0,87 ± 0,45 mm.

Conclusions: The high interobserver similarity of segmented LVs and delineated CTVs confirmed the robustness of the proposed method. Even an inexperienced user can perform a precise EAM-CT merge following workflow instructions.

Key words: ventricular tachycardia; radioablation; target delineation; intraobserver; interobserver

Introduction

Scar-related ventricular tachycardia (VT) is a potentially lethal complication of structural heart disease, and catheter ablation of the arrhythmogenic substrate is essential in complex therapeutic management [1]. However, catheter ablation can sometimes be limited because of inaccessible substrates (inability to reach epicardial surface or deep location within the wall or septum) [2]. Stereotactic arrythmia radioablation (STAR) is an alternative treatment method

for recurrent VTs after failed catheter ablation [3–5]. Compared with catheter ablation, STAR does not include substrate localization and must be performed by an electrophysiologist. Many factors can affect its overall accuracy, as has been well established by the treatment of malignant, benign, and functional diseases over many decades [6]. Important part of the current stereotactic arrythmia radioablation workflow is transfer of the electroanatomical study to computed tomography (CT) to be imported as secondary series to radiotherapy planning software and ensure maximum accuracy of target delineation

Several methods of target delineation have been proposed since the first VT patient was treated with STAR in 2012 [7]. The simplest approach involved manual contouring the clinical target volume (CTV) in the CT scan using exported images from an electroanatomic mapping (EAM) system and tagging the critical part of the arrhythmogenic substrate [8]. This method is clearly time-consuming and prone to error because of the subjective transfer of CTV from several three-dimensional (3D) visualizations to CT slices. Other techniques are based on merging maps with pre-procedural CT (secondary radiotherapy planning series) and following marking of the target [9–13]. In principle, two types of EAM-CT merge were proposed: manual alignment of EAM structures with segmented CT structures [9] or use of a semi-automatic algorithm [12].These methods, which require a fast intravenous bolus of contrast agent for CT, are gradually being improved, including the extension of EAM to other structures such as the left main coronary artery, coronary sinus, thoracic aorta, and chambers. This comprehensive approach offers the possibility of greater use of automated algorithms with the potential to reduce inaccuracies.

Here we analyzed inter- and intraobserver variation in a modified EAM-CT registration using automatic registration algorithms designed to yield higher robustness than non-automated approaches in the hands of inexperienced users.

Materials and methods

Patient selection

For this analysis, we selected 10 of 39 patients who had previously undergone STAR for scar-related VT after failed catheter ablation. Their EAM data were used for CTV definition under the supervision of two electrophysiologists. The location of the targets within the left ventricle (LV) covered more basal than apical segments (Fig. 1).

Electroanatomical data (EAM LV = left ventricle; EAM points = points with a specific tag for CTV delineation) were exported from CARTO software (CARTO® 3 system V6; Biosense

Webster, Diamond Bar, CA, US) and converted to a format (VTK- The Visualization Toolkit and FCSV- Fiducials Comma-Separated Values) compatible with 3D Slicer software (open source, www.slicer.org) using an in-house program written in C#. All patients had fast bolus contrast-enhanced CT (exhale breathhold, 1mm slice thickness, reduced field of view resulting in voxel size < 1 x 1 x 1 mm, 400 mA) from the time of STAR pre-treatment simulation. Registration of EAM and CT was performed using 3D Slicer (versions 4.8.1 and 4.10) following a previously published strategy [13] with significant modifications. The procedure is briefly described in **Figure 2 (see Supplementary File for details**).

Segmentation variability analysis

Two observers participated in this study. Observer 1 was an electrophysiologist technician from the cardiology department who was highly experienced in EAM-CT merge, CTV delineation, and anatomy of the heart, and the author of all modifications in the referenced procedure. Observer 2 was a clinical engineer from the oncology department, who was responsible for STAR treatment planning and minimally experienced with EAM-CT merge.

Both observers segmented LV from the CT image series for each case using a "grow from seeds" algorithm three times, with an interval of at least 8 h. Each segmentation was visually checked and manually adjusted if needed, in particular for features such as crossing sections with another structure and areas with metal artifacts from an implantable cardioverter defibrillator lead. The segmented LV CT was smoothed and the correction transformation applied to unify the CT coordinate system with EAM LV. Although CTVs cannot vary in volume (created from EAM data with a specific tag marking the STAR target area), the final position of the CTV within the LV could be affected by the precision of the CT LV segmentation and subsequent CT LV to EAM LV registration.

Variation was measured using the mean Hausdorff distance, Dice similarity coefficient (DSC), and absolute difference in center of gravity coordinates (CoG). The DSC represents the similarity of two 3D volumes in a range of 0-1 where 1 indicates a 100% match [14]. The Hausdorff mean distance is the mean distance between each point of one compared structure to the closest point in the other structure [15].

Intraobserver variability was considered as the first step in assessing the robustness of the proposed procedure. Observer 1, who had considerable experience in EAM-CT merge, performed the EAM-CT merge three times for each case, with an interval of at least 8 h. Intraobserver variability was evaluated using mean Hausdorff distance, DSC, and absolute

difference in CoG of segmented CT LVs and CTVs individually for each case and in total. Segmented CT LVs were compared with the relevant EAM LVs.

Observer 2, who had minimal experience with EAM-CT merge, performed the EAM-CT merge once for each patient following instructions written by observer 1 (see Supplementary File). Interobserver variability was evaluated by mean Hausdorff distance, DSC, and difference in CoG. We compared the first CT LV and the first CTV from observer 1 with the CT LV and CTV from observer 2.

Statistical analysis

Statistical analysis was performed using STATISTICA 13 software (StatSoft, Tulsa, OK, USA). All quantitative data were expressed as mean and standard deviation. To compare segmented LVs between the two observers, we used t-tests. Repeated-measures ANOVA was used to compare the trios of segmented LV volumes from observer 1. All tests were performed at the 5% level of significance.

Results

For observer 1, the similarity between CT LV and EAM LV was high (mean DSC of 0.84 ± 0.01), with a DSC of < 0.8 in only one case, in which CT was the poorest quality in the term of insufficient contrast agent within the LV (as a result of excesive inhomogenous endocardial hypertrabeculation and/or fibrotization). Contrast agent within LV was insufficient in this case, making segmentation more difficult and yielding a very irregular EAM LV. Table 1 shows the mean of absolute values of CoG differences, as averaging with negative values would have reduced the actual differences. When not using absolute values, we found that the mean differences for all cases were -0.23 mm, 0.08 mm, and 0.23 mm for X, Y, and Z coordinates, respectively, indicating no systematic error in any direction.

Intraobserver variability

The mean DSC was 0.92 ± 0.01 for all cases (30 in total, three comparisons for each case), indicating a high similarity of all segmented LVs (Tab. 2). Repeated-measures ANOVA confirmed no significant difference among three segmented LVs for each case ($p = 0.445$). The mean Hausdorf distance was 1.49 ± 0.23 for all cases, and the mean absolute difference in CoG coordinates was < 1.5 mm, also indicating good intraobserver agreement. The mean differences in CoG coordinates (without absolute values) for all cases were 0.69 mm, -0.04 mm, and -0.05 mm for the X, Y, and Z coordinates, respectively.

Table 3 shows the similarity and comparison of CTV localization for all cases (mean value of three EAM-CT merges for each case). The mean differences in CoG coordinates (without absolute values) for all cases were 0.16 mm, –0.1 mm, and –0.06 mm for X, Y, and Z coordinates, respectively, again indicating no systematic error in any direction.

DSC values for the comparison among CTVs was lower in all cases compared with DSC values among CT LVs. In contrast, the mean Hausdorf distance between CTVs was lower than for CT LVs. CTV was created from specific EAM points that were distributed in a surface area and did not vary much in the depth of the ventricle wall. In such cases where the object (CTV) is thin and planar (Figure 3), a small object translation can make a big difference in DSC, even if the mean Hausdorf distance remains low. Figure 3 shows an example of three CTVs with a mean DSC of 0.6 and mean Hausdorf distance of 1.19 mm.

Interobserver variability

Segmented CT LVs showed great similarity, with a mean DSC of 0.91 (range 0.88–0.94) for all cases. However, in the CTV comparison between observers, the mean DSC of all cases was 0.81 (range 0.66–0.94).

Interobserver differences in CT LV segmentation are reflected in different volumes of CT LVs, which can affect CoG and the corresponding CTV position after CT LV to EAM LV registration. CT LV volumes between both observers did not differ significantly (paired t-test $p = 0.06$), but difference in volumes correlated with DSC values for the compared CTVs (Pearson's correlation coefficient $R = 0.8$, $p = 0.005$).

Discussion

The precise transfer of EAM data into the radiotherapy planning CT is an important part of STAR in patients with scar-related VT after failed catheter ablation. We developed a modification of EAM-CT registration that ensures low intra- and interobserver variability using automatic algorithms. High robustness in overcoming incompatibility between the EAM and DICOM formats carries the prospect of precise targeting without unnecessarily increasing radiation volumes.

To date, different methods have been designed to merge EAM data with CT [8, 9, 1–13]. The simplest method is "indirect" target delineation, based on the manual contouring of CTV from several 3D visualizations to CT slices [8]. However, this method requires good anatomical knowledge and could be very operator dependent and time consuming.

This work was based on a previously published procedure [13], and our current goal was to modify the approach to be faster and more robust and involve minimal manual steps. In particular, we wanted to use specific EAM points to create a CTV model using an algorithm and to replace manual registration of EAM LV to CT LV. We also simulated a scenario in which EAM data contained only the LV and no other structures. The availability of EAM data for at least three chambers can yield a higher EAM-CT merge accuracy [9].

Comparison of segmented left ventricles with left ventricles from electroanatomical mapping showed high similarity between CT LV and EAM LV with DSC values of 0.84 ± 0.01 for observer 1 and 0.85 ± 0.04 for observer 2 and only one case with a DSC < 0.8. This singular case involved the poorest quality of CT with insufficient contrast agent within the LV, rendering segmentation difficult and yielding very irregular EAM LV. Kafi et al.[9] also published a method of EAM-CT merge using 3D Slicer software, but with more anatomical segments (cardiac cavities, ascending aorta, and pulmonary artery) and manual alignment of EAM data to CT. The target area was indicated on the surface of the EAM LV as 10 points, all manually connected. After projection of the target contour onto the CT images, observers drew a CTV throughout the LV wall thickness. For the EAM LV and CT LV, this group reported median DSC values of 0.86 (0.78–0.89) for observer 1 and 0.84 (0.82–0.88) for observer 2. These findings are comparable with our results.

To evaluate interobserver agreement we compared segmented CT LVs (mean Hausdorff distance of 1.86 mm, DSC 0.91) on which we moved the EAM LV using surface registration. Kafi et al. [9] evaluated interobserver agreement as median distance between EAM surfaces (2.6 mm) and DSC (0.86). We did not compare volumes of CTVs, which were exactly the same because we used only a set of EAM points with specific tags (marked during electroanatomical mapping). Comparison of CTV similarity between observers showed a mean DSC of 0.81 ± 0.11 and mean Hausdorff distance for all cases of 1.18 ± 1.11 (Tab. 4). We created CTV from marked points on the EAM map, so from this perspective, comparison of our CTVs is a subset of EAM comparisons. Kafi et al. [9] compared the target surface area of interest and volume of CTV. Finally, the median distance among the 10 points (area of interest) was 7 mm (4.3–10 mm) for both observers in their study.

Our data from both observers for all cases altogether showed a mean Hausdorf distance of 3.2 mm (95th percentile, 7.95 mm) for the EAM map to the CT LV and a DSC of 0.84 between the EAM LV and CT LV. Hohmann et al. [12] published a similar method of EAM-CT merge, with a merge process based on manual alignment followed by automated registration using an iterative closest point algorithm (with the LV and thoracic aorta as

anatomic landmarks) in 3D Slicer software. For one case, they reported a mean pointwise distance of 3.1 mm (95th percentile, 8.3 mm) for the EAM map to the CT LV endocardial surface and a DSC of 0.83 between the EAM map of the LV and corresponding CT LV.

Brett et al. [11] proposed a workflow for conversion of EAM to DICOM files that requires several manual steps, including placing fiducials to mark the target. This technique relies heavily on the identification of anatomic landmarks. Their method allows for higher precision than an indirect approach, but they did not report intra/interobserver variability or the associated reproducibility rate.

During the conducting of this work two other publications addressing the same issue were produced. Wang et al. [16] built a plug-in module on the 3D Slicer platform. Registration of EAM to cardiac MR/CT data starts with manually placing landmark pairs requiring certain anatomical knowledge. No reproducibility of target delineation is described here. Oh et al. [17] developed an in-house software to read EAM maps, registered them to a planning image set and converted them to DICOM files. A total of 7 patients underwent STAR treatment by defining the target with the proposed method. The authors reported DSC of 0.814 ± 0.053 between the EAM LV and CT LV from 7 cases. The target location on 3D space was inconsistent with no clear trend in terms of similarity but the authors compared the clinical target from EAM with the target defined by 17-segment model [18].

Our results demonstrate that we can achieve DSCs of 0.95 and 0.93 for intraobserver comparisons of multiple segmented CT LVs and created CTVs. Similarly, we achieved DSCs of 0.94 and 0.95 for interobserver comparison of segmented CT LV and created CTVs. The fact that observer 2 had only a basic knowledge of heart anatomy from radiotherapy planning underscores the robustness of the proposed procedure. Such results were achieved in cases where the chamber was well defined on contrast CT.

We did find DCS values of 0.6 and 0.66 in the intra- and interobserver comparison of CTVs (the worst cases). The AAPM guideline[19] recommends a DSC of 0.8–0.9 for testing of deformable image registration performance. DSC calculations depend on the volume of a structure so that very large or very small structures may have different expected DSC values for contour uncertainty. As shown in Figure 3, if EAM points for creation of CTV are distributed almost on the same plane, even a small shift will yield a significant difference in the DSC, whereas mean Hausdorff distance will remain low.

Our study is limited by the use of EAM from endocardial mapping, and we did not test our procedure using EAM from epicardial access. All EAM data were exported from the CARTO® 3 system. The weakest step of our procedure is the manual segmentation, which

influences the final localization of the CTV. Although EAM inherently cannot generate a perfect model of the LV, as Table 1 shows, a high similarity between CT LV and EAM LV is possible. Our method is fast and can be completed within 10–15 minutes, with results that are equivalent to or better than those previously reported.

Worth noting is that good intra- or interobserver agreement does not guarantee correct localization of the CTV within the heart. The big advantage of our method is elimination of all manual shifts for any of the structures. We believe that manually moving the EAM LV or EAM points could be a significant source of potential error. Also worth noting is that the quality of the LV segmentation affects the position of CTV using our method. In addition, with this method, we delineate the CTV only according to the given EAM points. For STAR purposes, the CTV must be expanded throughout the LV wall thickness. This step is not a part of our method, and the final CTV is created in the radiotherapy planning system by a radiation oncologist.

Conclusion

The high interobserver similarity of segmented LVs and delineated CTVs confirmed the robustness of the proposed method. Even an inexperienced user can perform a precise EAM-CT merge following our workflow instructions. Accurate segmentation of LV is crucial for successful, precise CTV delineation.

References

1. Cronin E, Bogun F, Maury P, et al. 2019 HRS/EHRA/APHRS/LAHRS expert consensus statement on catheter ablation of ventricular arrhythmias. EP Europace. 2019; 21(8): 1143–1144, doi: 10.1093/europace/euz132.

2. Tokuda M, Kojodjojo P, Tung S, et al. Acute failure of catheter ablation for ventricular tachycardia due to structural heart disease: causes and significance. J Am Heart Assoc. 2013; 2(3): e000072, doi: 10.1161/JAHA.113.000072, indexed in Pubmed: 23727700.

3.   Haskova J, Sramko M, Cvek J, et al. Stereotactic Radiotherapy in the Management of Ventricular Tachycardias: More Questions than Answers? Card Electrophysiol Clin. 2022; 14(4): 779–792, doi: 10.1016/j.ccep.2022.06.010, indexed in Pubmed: 36396193.

4.   Grehn M, Mandija S, Miszczyk M, et al. STereotactic Arrhythmia Radioablation (STAR): the Standardized Treatment and Outcome Platform for Stereotactic Therapy Of Re-entrant tachycardia by a Multidisciplinary consortium (STOPSTORM.eu) and review of current patterns of STAR practice in Europe. Europace. 2023; 25(4): 1284–1295, doi: 10.1093/europace/euac238, indexed in Pubmed: 36879464.

5.   van der Ree MH, Blanck O, Limpens J, et al. Cardiac radioablation-A systematic review. Heart Rhythm. 2020; 17(8): 1381–1392, doi: 10.1016/j.hrthm.2020.03.013, indexed in Pubmed: 32205299.

6.   Seuntjens J. Prescribing, Recording, and Reporting of Stereotactic Treatments with Small Photon Beams, ICRU 2017; Report 91 (No. IAEA-CN--250). 2017.

7.   Loo BW, Soltys SG, Wang L, et al. Stereotactic ablative radiotherapy for the treatment of refractory cardiac ventricular arrhythmia. Circ Arrhythm Electrophysiol. 2015; 8(3): 748–750, doi: 10.1161/CIRCEP.115.002765, indexed in Pubmed: 26082532.

8.   Neuwirth R, Cvek J, Knybel L, et al. Stereotactic radiosurgery for ablation of ventricular tachycardia. Europace. 2019; 21(7): 1088–1095, doi: 10.1093/europace/euz133, indexed in Pubmed: 31121018.

9.   Abdel-Kafi S, Sramko M, Omara S, et al. Accuracy of electroanatomical mapping-guided cardiac radiotherapy for ventricular tachycardia: pitfalls and solutions. Europace. 2021; 23(12): 1989–1997, doi: 10.1093/europace/euab195, indexed in Pubmed: 34524422.

10. Abdel-Kafi S, de Ridder M, de Riva M, et al. Integration of Electroanatomical Mapping With Imaging to Guide Radiotherapy of VT Substrates With High Accuracy. JACC Clin Electrophysiol. 2020; 6(7): 874–876, doi: 10.1016/j.jacep.2020.03.014, indexed in Pubmed: 32703572.

11. Brett CL, Cook JA, Aboud AA, et al. Novel workflow for conversion of catheter-based electroanatomic mapping to DICOM imaging for noninvasive radioablation of ventricular tachycardia. Pract Radiat Oncol. 2021; 11(1): 84–88, doi: 10.1016/j.prro.2020.04.006, indexed in Pubmed: 32416269.

12. Hohmann S, Henkenberens C, Zormpas C, et al. A novel open-source software-based high-precision workflow for target definition in cardiac radioablation. J Cardiovasc Electrophysiol. 2020; 31(10): 2689–2695, doi: 10.1111/jce.14660, indexed in Pubmed: 32648343.

13. Peichl P, Sramko M, Cvek J, et al. A case report of successful elimination of recurrent ventricular tachycardia by repeated stereotactic radiotherapy: the importance of accurate target volume delineation. Eur Heart J Case Rep. 2021; 5(2): ytaa516, doi: 10.1093/ehjcr/ytaa516, indexed in Pubmed: 33598611.

14. Zhu Ji, Chen X, Yang B, et al. Evaluation of Automatic Segmentation Model With Dosimetric Metrics for Radiotherapy of Esophageal Cancer. Front Oncol. 2020; 10: 564737, doi: 10.3389/fonc.2020.564737, indexed in Pubmed: 33117694.

15. Huttenlocher DP, Klanderman GA, Rucklidge WJ. Comparing images using the Hausdorff distance. IEEE Transactions on Pattern Analysis and Machine Intelligence. 1993; 15(9): 850–863, doi: 10.1109/34.232073.

16. Wang H, Barbhaiya CR, Yuan Ye, et al. A Tool to Integrate Electrophysiological Mapping for Cardiac Radioablation of Ventricular Tachycardia. Adv Radiat Oncol. 2023; 8(6): 101272, doi: 10.1016/j.adro.2023.101272, indexed in Pubmed: 37415904.

17. Oh S, Liu EH, Trombetta MG, et al. A target definition based on electroanatomic maps for stereotactic arrhythmia radioablation. Phys Med. 2023; 115: 103160, doi: 10.1016/j.ejmp.2023.103160, indexed in Pubmed: 37847954.

18. Brownstein J, Afzal M, Okabe T, et al. Method and Atlas to Enable Targeting for Cardiac Radioablation Employing the American Heart Association Segmented Model. Int J Radiat

Oncol Biol Phys. 2021; 111(1): 178–185, doi: 10.1016/j.ijrobp.2021.03.051, indexed in Pubmed: 33836242.

19. Brock KK, Mutic S, McNutt TR, et al. Use of image registration and fusion algorithms and techniques in radiotherapy: Report of the AAPM Radiation Therapy Committee Task Group No. 132. Med Phys. 2017; 44(7): e43–e76, doi: 10.1002/mp.12256, indexed in Pubmed: 28376237.

Table 1. Comparison of segmented left ventricles with left ventricles from electroanatomical mapping to evaluate intraobserver variability for observer 1

CT LV *vs.* EAM LV					Center of gravity coordinates difference [mm]		
Patient	DSC*	SD	Mean Hausdorf distance [mm]*	SD	X**	Y**	Z**
1	0.88	0.01	2.63	0.23	0.69	1.09	0.66
2	0.88	0.00	2.53	0.08	0.80	1.07	1.07
3	0.86	0.03	2.88	0.43	1.63	1.50	0.17
4	0.83	0.01	3.43	0.12	0.83	1.15	1.19
5	0.82	0.02	3.23	0.27	0.34	0.39	0.80
6	0.80	0.01	3.73	0.13	1.50	0.76	1.20
7	0.85	0.02	3.04	0.58	2.10	1.19	1.04
8	0.85	0.01	3.11	0.15	0.71	0.98	1.24
9	0.86	0.02	3.08	0.50	1.29	1.56	1.18
10	0.76	0.02	4.71	0.60	2.51	1.92	1.32
Mean	**0.84**	**0.01**	**3.24**	**0.31**	**1.24**	**1.16**	**0.99**

*mean value of Dice similarity coefficient (DSC) from three segmentations

**mean of the absolute value of coordinate differences from three segmentations

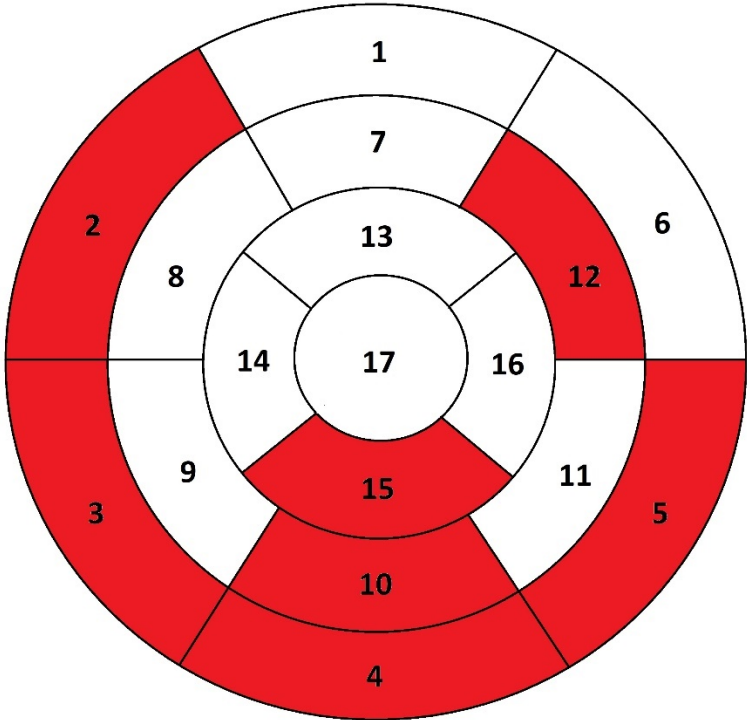CT — computed tomography; LV — left ventricle; EAM — electroanatomic mapping; SD — standard deviation

Table 2. Comparison among three segmented left ventricles (LVs) for each case to evaluate intraobserver variability and reproducibility of LV segmentation over time

Intraobserver variability CT LV					Center of gravity coordinates difference [mm]		
Patient	DSC*	SD	Mean Hausdorf distance [mm]*	SD	X**	Y**	Z**
1	0.94	0.01	1.22	0.08	0.18	0.78	0.20
2	0.94	0.01	1.38	0.10	1.47	1.28	0.50
3	0.94	0.02	1.26	0.26	1.24	1.09	0.63
4	0.93	0.01	1.39	0.25	0.77	1.63	0.73
5	0.92	0.01	1.12	0.10	1.34	1.27	1.04

6	0.94	0.01	1.08	0.18	0.56	0.93	1.36
7	0.90	0.02	1.88	0.38	2.31	1.29	1.16
8	0.95	0.01	0.98	0.17	0.75	0.23	0.50
9	0.89	0.01	2.41	0.15	2.56	0.79	2.79
10	0.89	0.03	2.16	0.64	2.21	2.64	1.20
Mean	**0.92**	**0.01**	**1.49**	**0.23**	**1.34**	**1.19**	**1.01**

*mean value of Dice similarity coefficient from three segmentations

**mean of the absolute value of coordinate differences from three segmentations

CT — computed tomography; EAM — electroanatomic mapping; SD — standard deviation

Table 3. Comparison of three delineated clinical target volumes (CTVs) for each case to evaluate intraobserver variability for observer 1

Intraobserver variability CTV							
					Center of gravity coordinates difference (mm)		
Patient	DSC*	SD	Mean Hausdorf distance (mm)*	SD	X**	Y**	Z**
1	0.60	0.19	1.19	0.59	1.10	1.04	1.69
2	0.88	0.03	0.82	0.24	1.27	1.87	0.40
3	0.84	0.03	0.37	0.07	0.80	0.59	0.25
4	0.91	0.02	0.51	0.07	0.21	0.78	0.57
5	0.90	0.02	0.73	0.13	0.81	0.98	0.21
6	0.93	0.02	0.50	0.08	0.13	0.51	0.42
7	0.89	0.02	0.50	0.09	0.32	0.87	0.81
8	0.87	0.05	0.77	0.28	0.60	1.22	1.07
9	0.71	0.10	1.23	0.45	0.42	0.93	1.77
10	0.71	0.09	0.51	0.15	0.72	0.75	0.58
Mean	**0.82**	**0.06**	**0.71**	**0.22**	**0.64**	**0.95**	**0.78**

*mean value of Dice similarity coefficient (DSC) from three segmentations

**mean of the absolute value of coordinate differences from three segmentations

CT — computed tomography; EAM — electroanatomic mapping; SD — standard deviation

Table 4. Comparison of interobserver variability between observers 1 and 2 in segmented left ventricles (LVs) and delineated clinical target volumes (CTVs)

Interobserver variability											
Comparison of CT LV							Comparison of CTV				
Patient	DSC	Mean Hausdorf	X*	Y*	Z*	Δ Volume	DSC	Mean Hausdorf	X*	Y*	Z*

		distance [mm]				CT LV [cm³]		distance [mm]			
1	0.93	1.45	0.74	0.26	0.37	9.54	0.89	0.39	0.51	0.11	0.12
2	0.93	1.52	0.29	0.08	0.13	3.56	0.94	0.48	1.23	0.27	0.16
3	0.92	1.67	0.49	0.40	0.22	24.88	0.68	0.80	2.07	0.58	1.28
4	0.92	1.79	0.54	1.39	0.21	27.48	0.71	1.59	0.05	3.26	0.81
5	0.88	1.98	0.18	1.80	1.89	2.12	0.89	0.85	0.21	0.75	1.79
6	0.92	1.57	2.87	2.68	0.72	2.04	0.84	1.17	1.75	2.01	1.60
7	0.88	2.66	0.18	2.76	1.41	43.32	0.74	1.31	2.60	2.31	2.11
8	0.94	1.33	1.00	0.66	0.62	13.39	0.95	0.32	0.22	0.07	0.15
9	0.89	2.65	1.46	1.93	1.60	38.40	0.66	1.29	3.02	1.27	0.34
10	0.92	1.93	0.49	2.64	0.53	28.73	0.78	0.46	0.14	0.70	1.36
Mean	**0.91**	**1.86**	**0.82**	**1.46**	**0.77**		**0.81**	**0.87**	**1.18**	**1.13**	**0.97**

*Absolute value of coordinate difference

DSC — Dice similarity coefficient CT — computed tomography; SD — standard deviation

Figure 1. Location of individual targets within the left ventricle using a 17-segment heart model (target located in segment 4 in four cases)
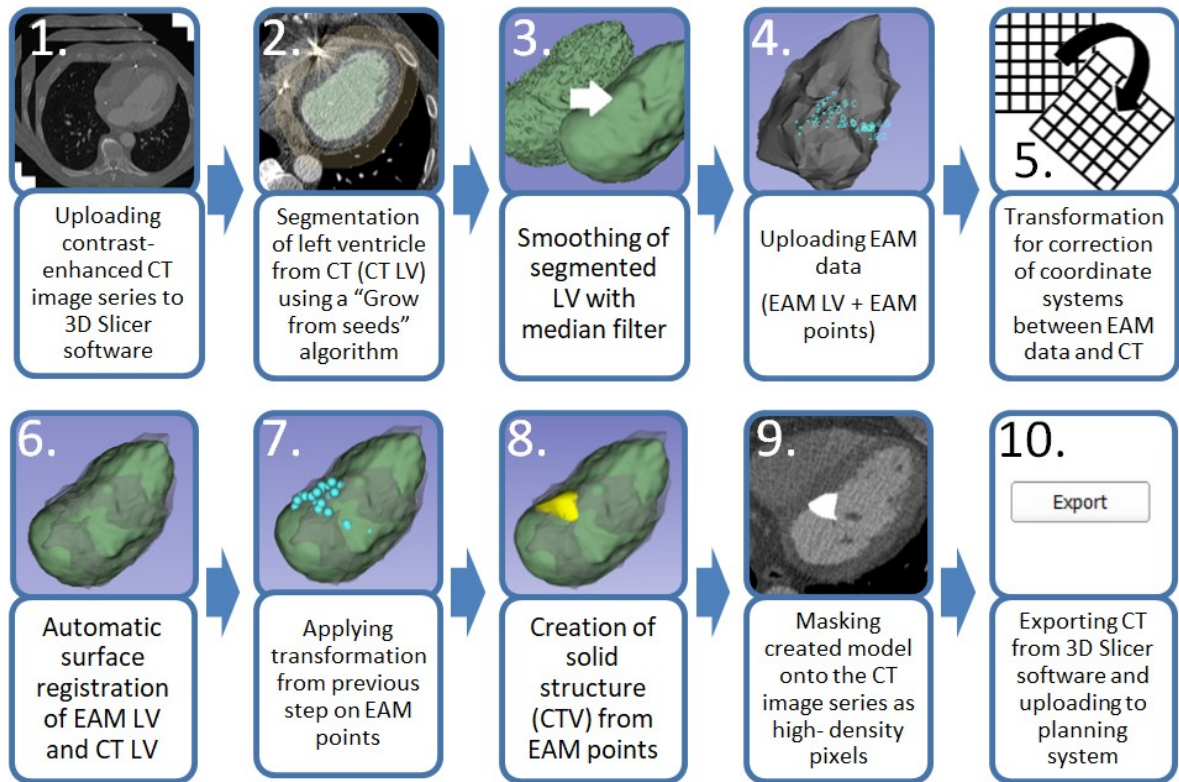
Figure 2. Visual presentation of the electroanatomic mapping–computed tomography (EAM-CT) merge procedure
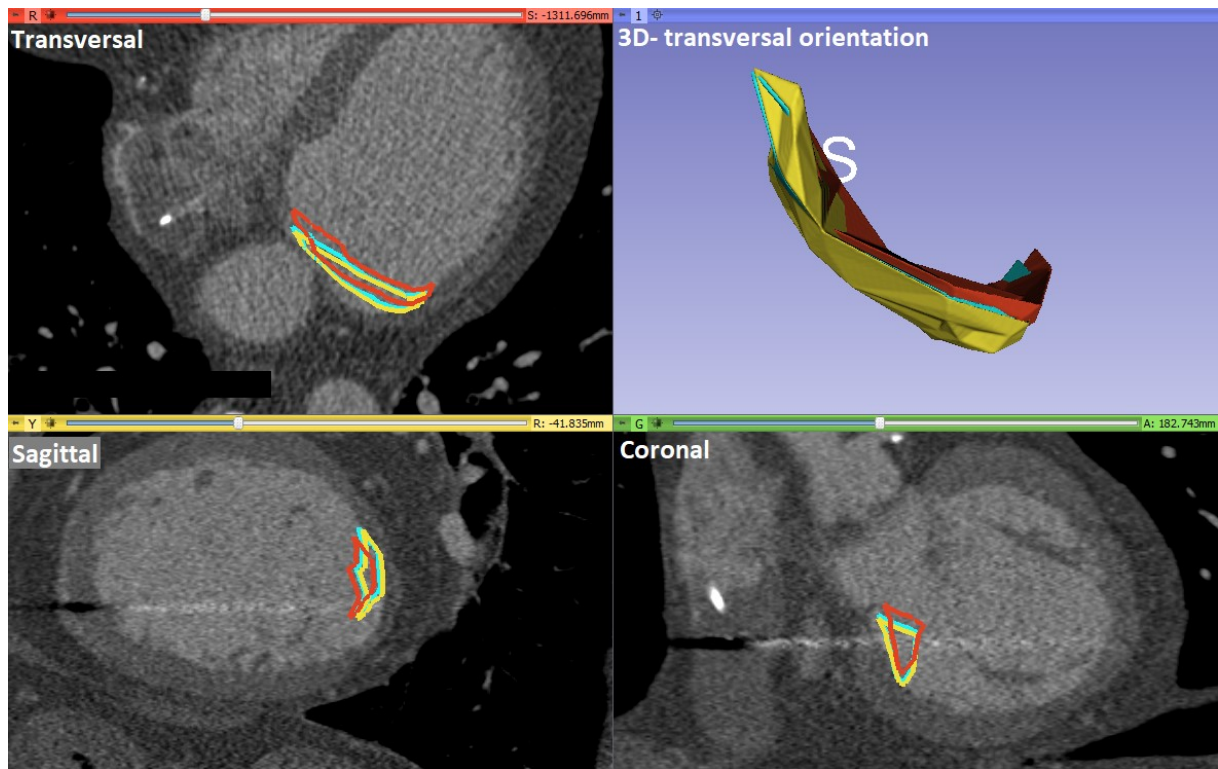
Figure 3. Example of three clinical target volumes (CTVs) delineated at least 8 hours apart, with the worst Dice coefficient from all cases
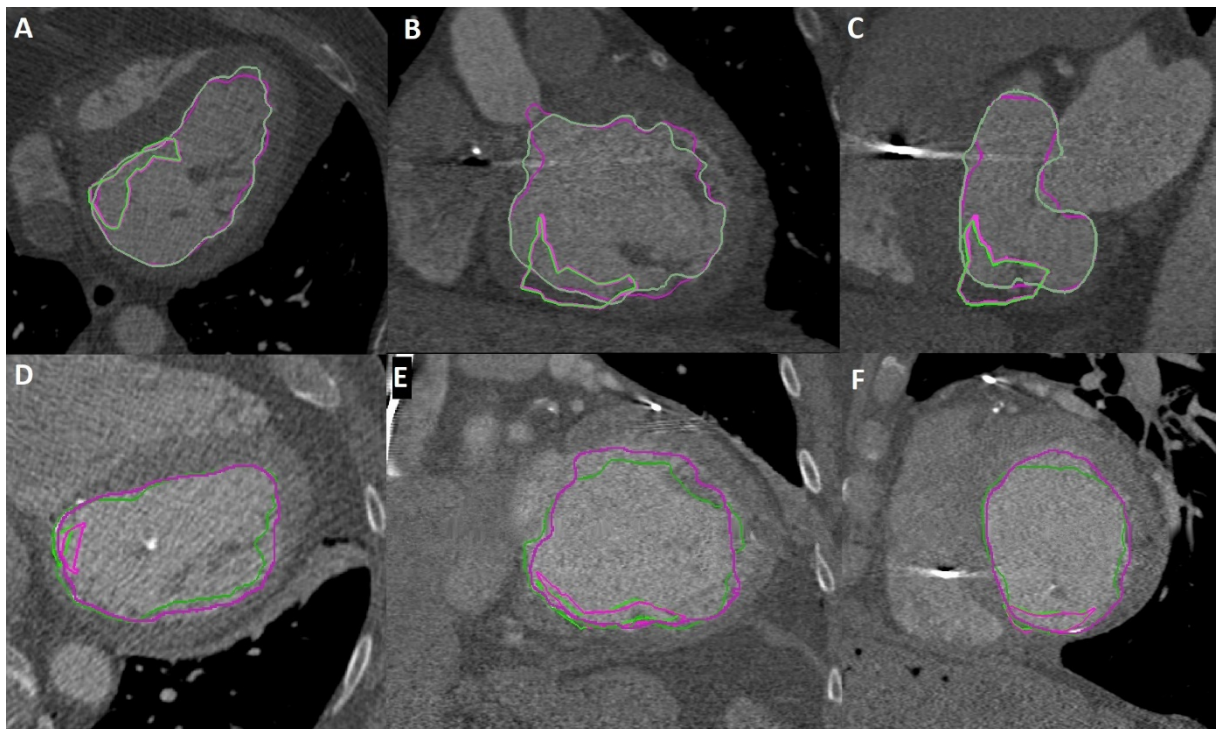
Figure 4. Examples of the best and worst interobserver agreement values for segmented LVs and delineated CTVs: LVs and CTVs from case 8 (DSC of 0.94 for LVs and 0.95 for CTVs) in transversal (A), coronal (B), and sagittal (C) planes (green = observer 1 , pink = observer 2); and LVs and CTVs from case 9 (DCS of 0.89 for LVs and 0.66 for CTVs) in (D) transversal, (E) coronal, and sagittal (F) planes (green = observer 1 , pink = observer 2)

Supplementary File

Instructions for performing an EAM-CT merge in 3D Slicer
This supplement describes our EAM-CT merge method in more detail. You will need 3D Slicer software, which is freely available (www.slicer.org).
1)   **Uploading contrast-enhanced CT image series to 3D Slicer software**
   a.   Use "DICOM browser" to **Import** and **Load** the relevant CT series.
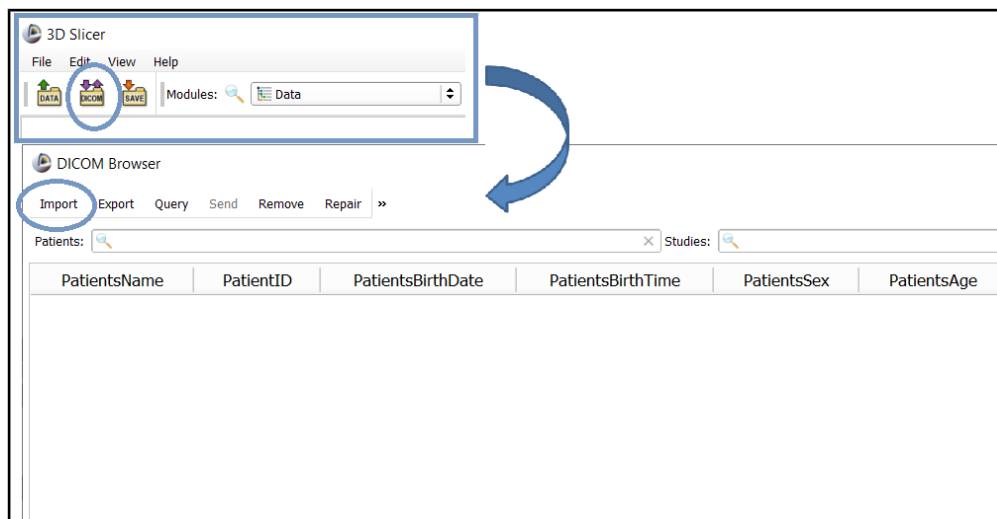
   b.   When the CT is uploaded, adjust contrast with the left mouse button or use the **Volumes** module where several Window/Level presets are available.
   c.   For contrast-enhanced CT, we usually start with W600-1000/L200-400 and perform manual adjustments with the left mouse button to increase the difference between the left ventricle (LV) with contrast agent and surrounding tissue.
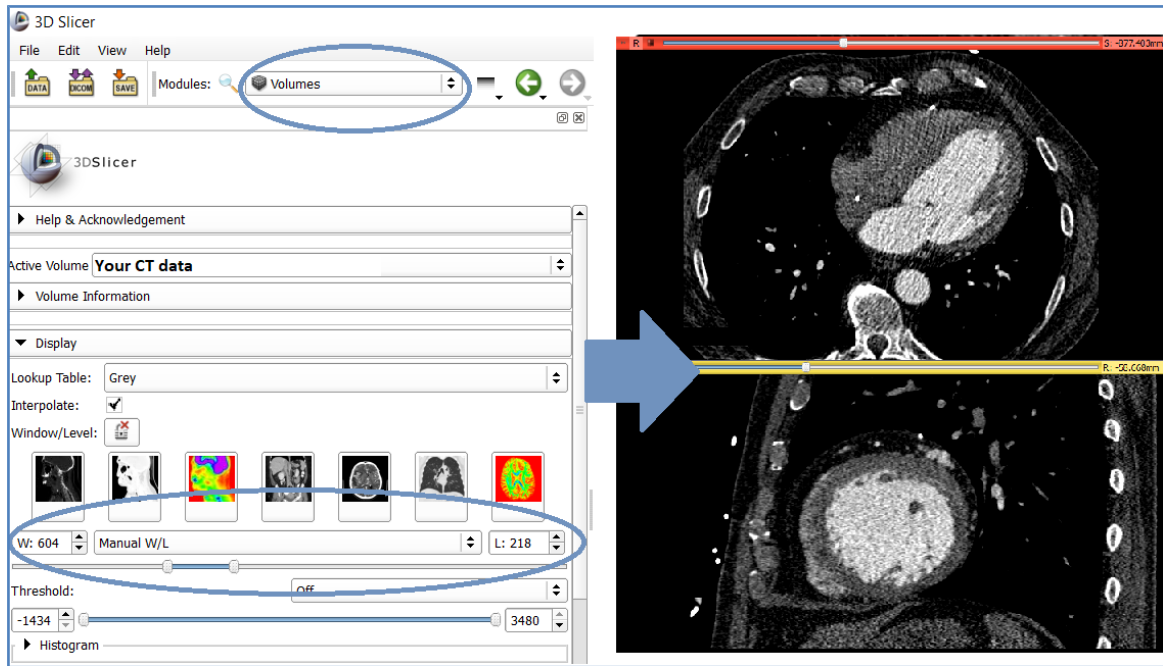
2) **Segmentation of LV from CT (CT LV)**

    a. Choose **Segment Editor** from the drop-down menu. Select your CT as **Master volume** if not selected automatically.

    b. Use the **+ADD** button to make two new segments. We renamed the defaults as **Contrast** (for the LV) and **Outside**.
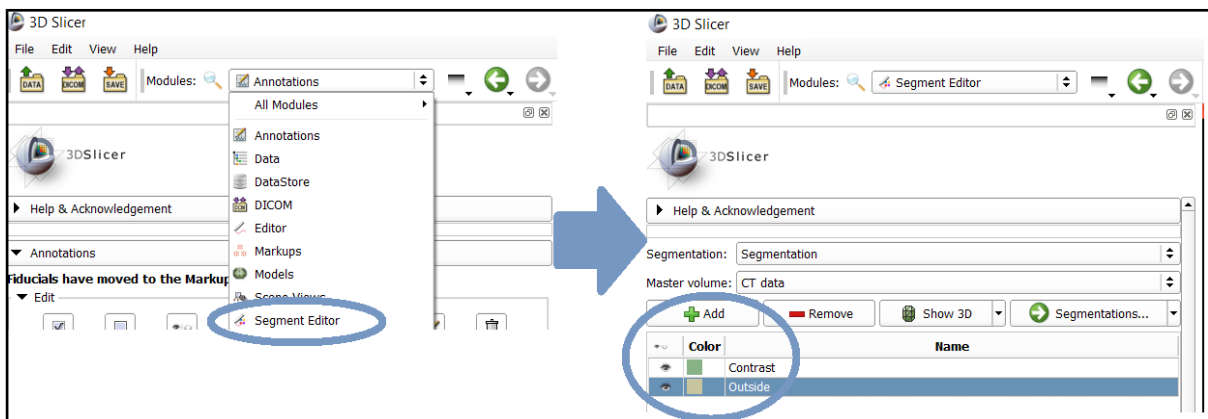

    c. For **Contrast** segment, mark several points inside the left ventricle using the **Paint** effect.

    d. Mark some points within LV in all planes (transversal, coronal, sagittal).

    e. For **Outside** segment, mark several points that will clearly indicate what is outside the LV.

    f. All of these marked areas will serve as "SEEDS" for the "**grow from seeds**" algorithm.

Tips: mark border between atrium and ventricle; border between aorta and LV; carefully check areas with artifacts and electrodes.
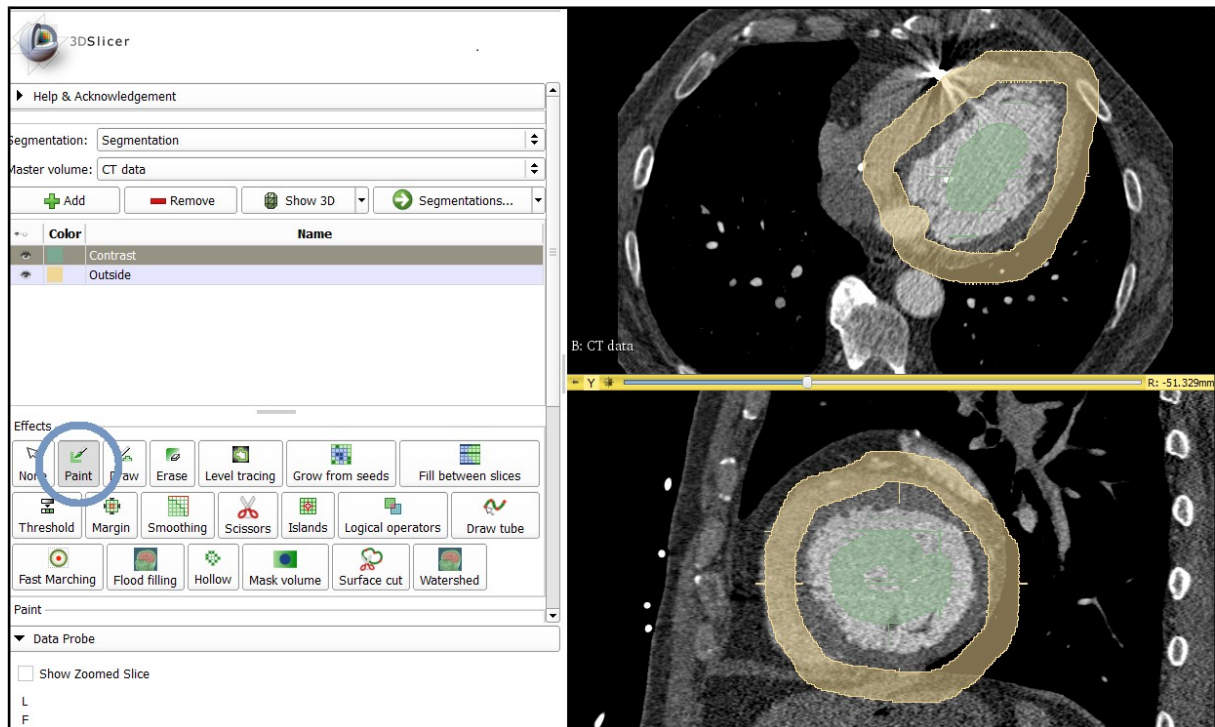
g. Select **Grow from seeds** in the Segmentation Module and Initialize. This process takes a few seconds or minutes (based on your PC performance).
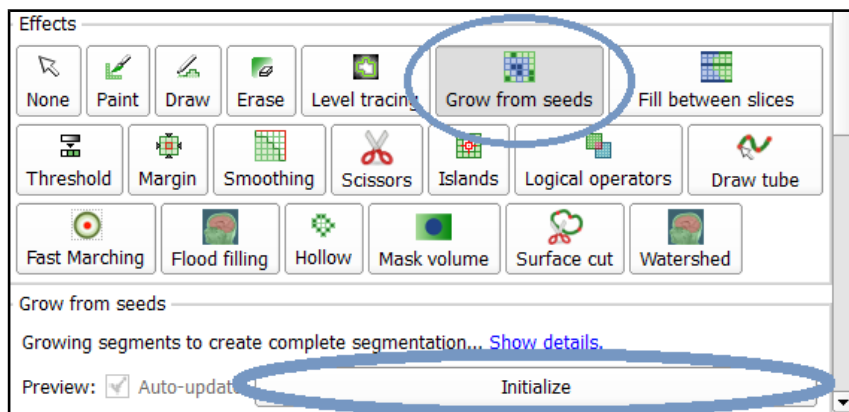
h. Select **Segmentation** as **Segmentation preview**.

i. Choose **Master Volume** as your CT data.

j. Select "Show 3D" and UNcheck "Outside" segment (the eye symbol) – now you can see your segmented LV in all planes and 3D.

*Note: In this step, it is useful to check segmentation in all slices and, if needed, perform manual fine adjustments with the **Paint** or **Erase** tools under the **Effects** tab.*
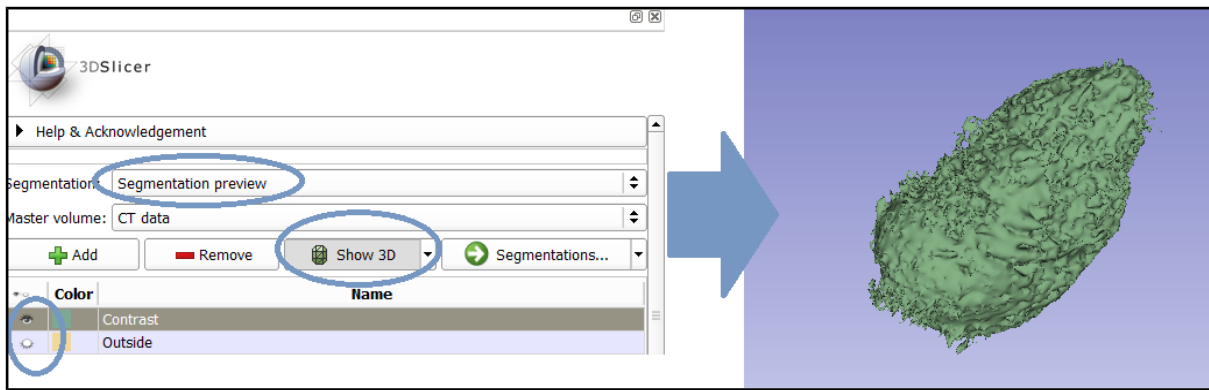
3) **Smoothing of the segmented LV with median filter**

    a. Still in **Segmentation Preview**, select the **Islands** effect, and under the **Islands** tab choose **Keep the largest island** and select **Apply** (this step removes small connected components created during the "Grow from seeds" step).
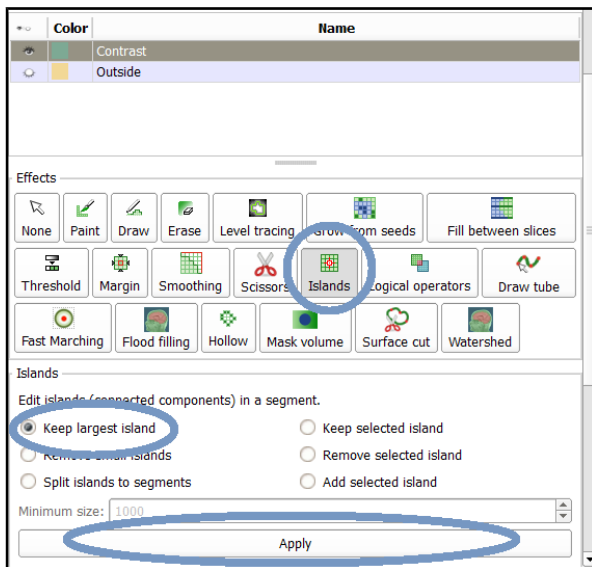
    b. Select the **Smoothing** effect.

    c. **Smoothing method**: Median; **Kernel Size**: 5 mm (more details about the filter are at the end of this Supplement).
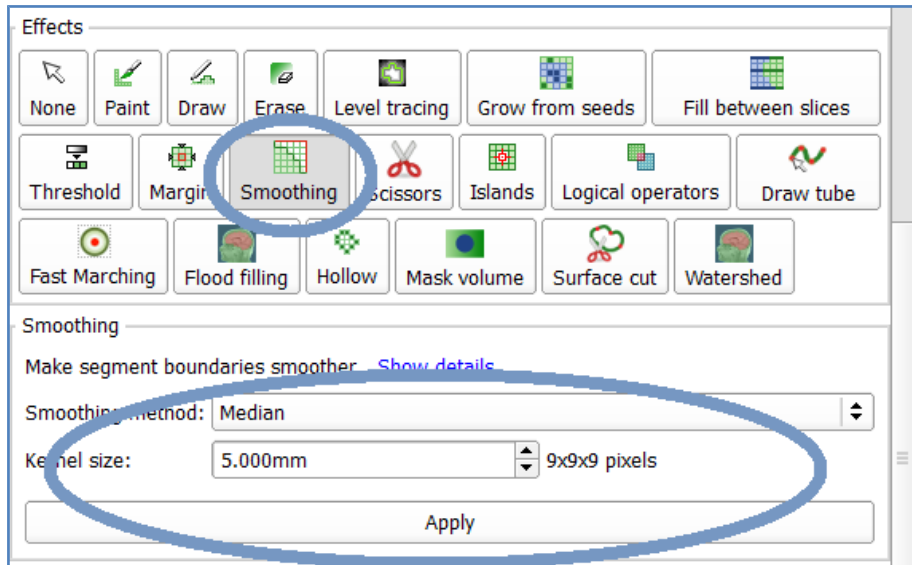
Now, you have completed segmentation of the LV.

    d. Choose the **Data** module from the drop-down menu.

    e. Select **Segmentation preview**, press the right mouse button, and select **Export visible segments to models**. The segmented LV will change to a model.
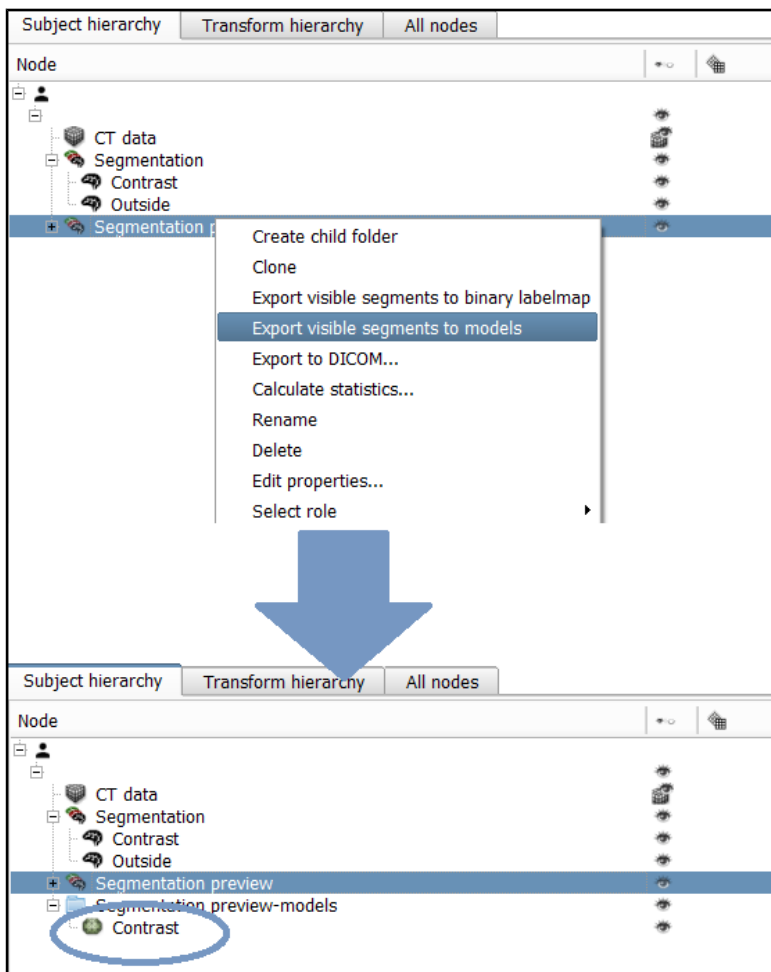
4) Uploading EAM data (left ventricle = EAM LV, points with specific tag for GTV delineation)

    a. For next steps, it is necessary to load additional data:

- File with transformation for correction of coordinate systems (this file, *CT2EAM_transformation*, is part of this Supplement)
- EAM data – map of the LV and specific points indicating the target area (***EAMmodel, EAMpoints*** in these instructions)

Note: EAM data in this work were exported from CARTO software (CARTO® 3 system (Biosense Webster, Diamond Bar, CA, US) and converted to a format compatible with 3D Slicer software (open source,) using an in-house program written in C# (we can share this code upon request).

    b. For data import, select **Data** in the top left corner of the screen, select **Choose File(s) to Add**, and choose your folder with data, or simply drag and drop these files from the specific folder to 3D Slicer. Another window will appear with a description of files being loaded – Transform, Model, MarkupsFiducial (3D Slicer usually recognizes the correct type).
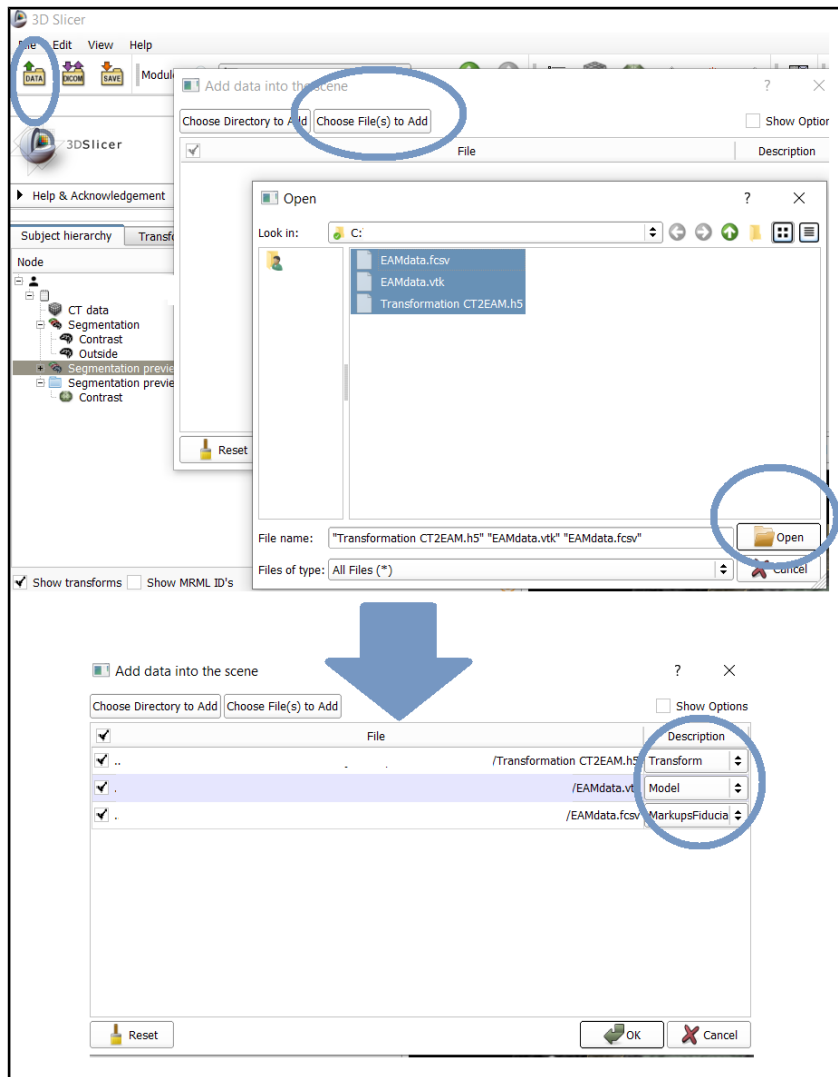
5)   Applying transformation for correction of coordinate systems between EAM data and CT

After loading of EAM data into 3D Slicer, you can see in the 3D view the different positions and orientations of the segmented LV and EAM data (model and points). The correction transformation will unify different orientations (90° rotation in SI direction and 180° rotation in AP direction).
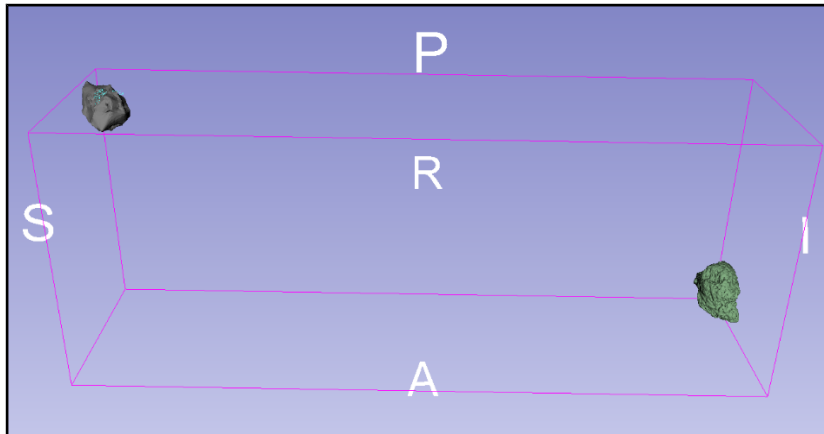
5.1.) 3D Slicer version > 4.10

    a. Select EAMmodel in the **Data** module, press the right mouse button, and choose the relevant **Transformation**. A symbol of applied transformation (grid) will appear on the right in the **Data** module.

    b. Again, press the right mouse button and choose **Harden Transform** to permanently fix transformation.

    c. Repeat the same steps for EAMpoints.
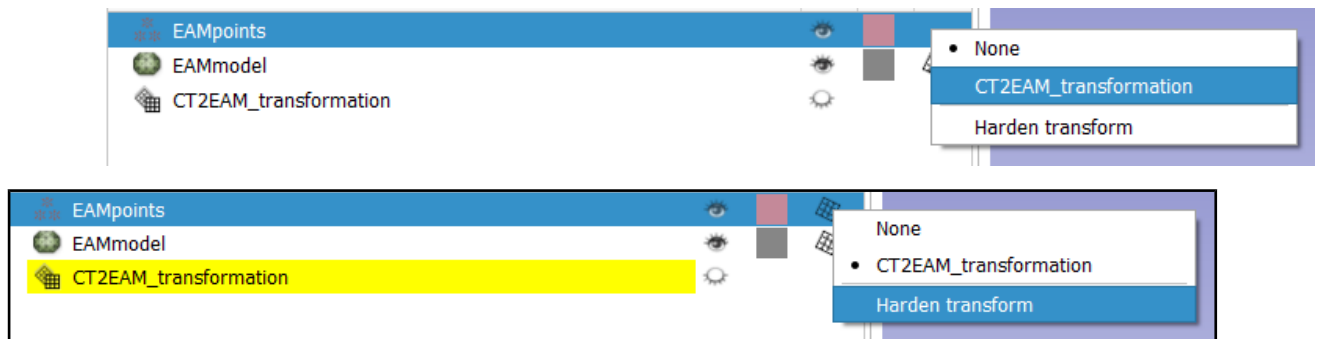
5.2.) 3D Slicer version < 4.10

    a. Choose the **Transforms** module from the drop-down menu and select the relevant transformation as **Active Transform**.

    b. At the bottom of this module, select EAMmodel and EAMpoints and apply the active transform to the selected transformable node by clicking on the **arrow icon**.

    c. With EAMmodel selected in the **Transformed** window, harden the transform by clicking on the **transform icon** (EAMmodel and EAM points will be back in the Transformable window with the new orientation).
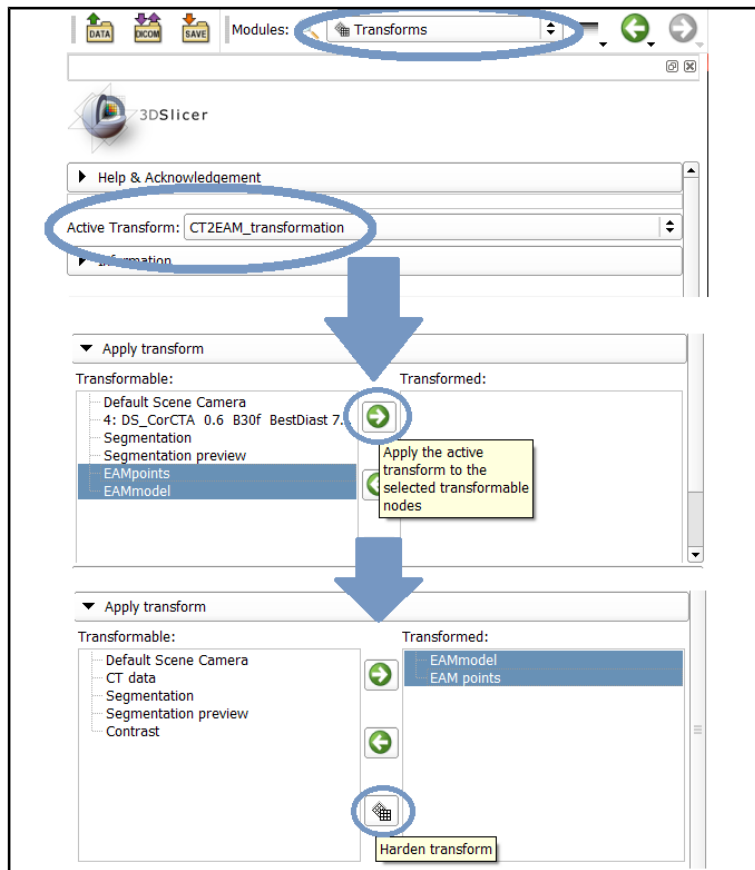
6) **Automatic surface registration of EAM LV and CT LV**

    a. Choose the **Surface Registration** module from the drop-down menu (or search "module" with the magnifying glass symbol).

    b. **Inputs tab**: select the model of segmented LV as the **Fixed Model** and EAMmodel as the **Moving Model**.

    c. **Outputs tab**: select **Create new linear transform** as the **Output Transform** (you can rename the new transform).
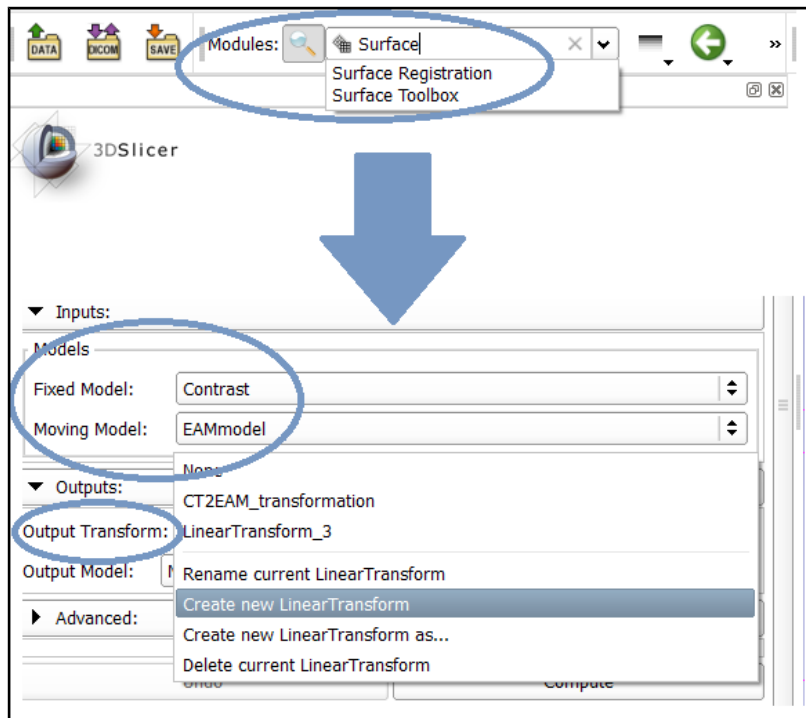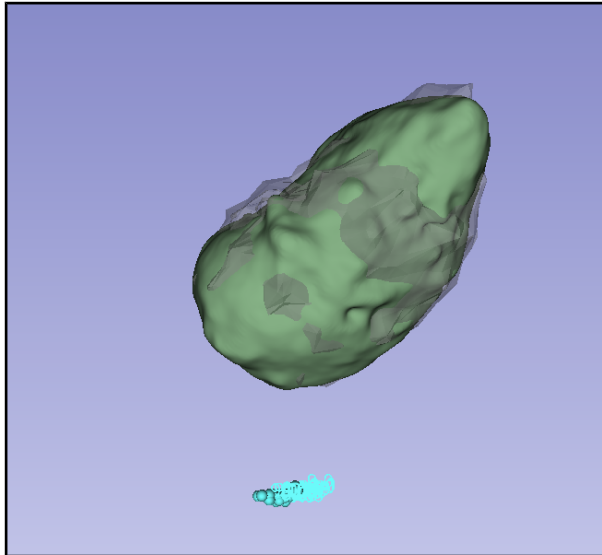
d. Advanced tab:

- **Fiducial Transform Mode:** Rigid Body
- **Mean Distance Mode**: Root Mean Square
- Check the **Start by matching centroids** checkbox.
- Check the **Check Mean Distance** checkbox.
- Select **Compute**.
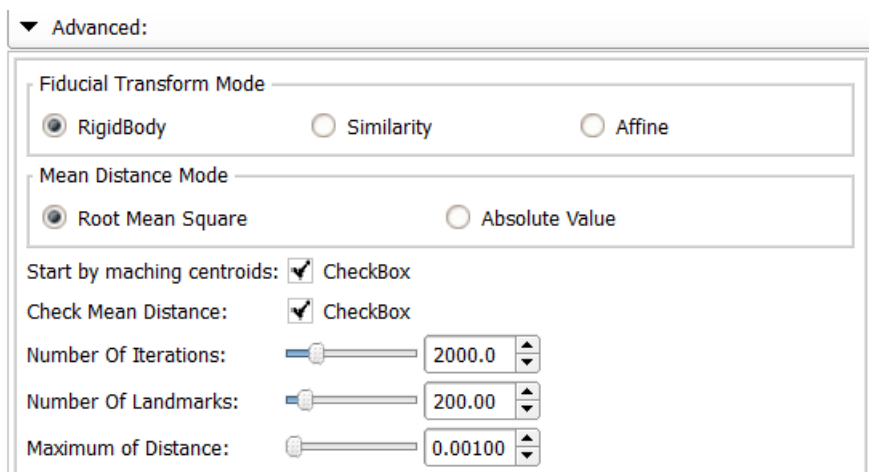
After successful computation, you will see the EAMmodel and LV model overlapping each other (EAMpoints are not affected and will be still away).

**7)   Applying transformation from the previous step on EAM points representing GTV**

It is necessary to harden the new transform applied on the EAMmodel and also apply and harden this transform on EAMpoints.

  a. Based on the 3D Slicer version, follow the same steps as mentioned in Step 5 with the transformation created in Step 6c.

  b. After this step, EAMpoints, EAMmodel, and the segmented model of LV will be

merged.
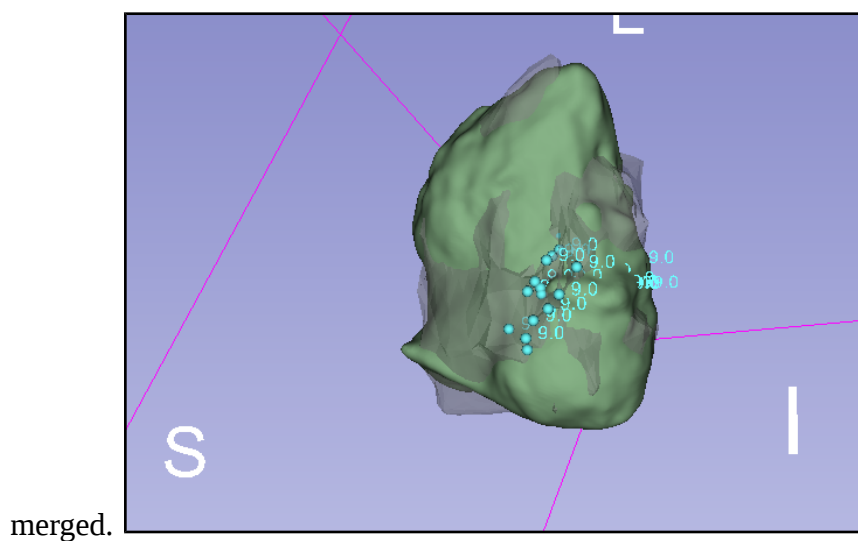
8) Creation of solid structure (GTV) from EAM points with specific tags

   a. Choose **Markups to Model** module from the drop-down menu (or search "module" with the magnifying glass symbol).

   b. **Model type**: Closed Surface.

   c. Select EAMpoints as **Input node**.

   d. Output model: choose **Create new model**.

   e. Closed Surface Model tab: Uncheck **Clean Duplicate Input Points**, **Smoothing**, and **Force convex output**.

   f. Set **Convexity** to 5–20. If the value is 0, then a convex shape is created. The larger the value, the more convex the generated surface is. Our experience shows that the chosen value depends on the spacing and number of points forming the model. Choose a value that makes the resulting model match your idea.
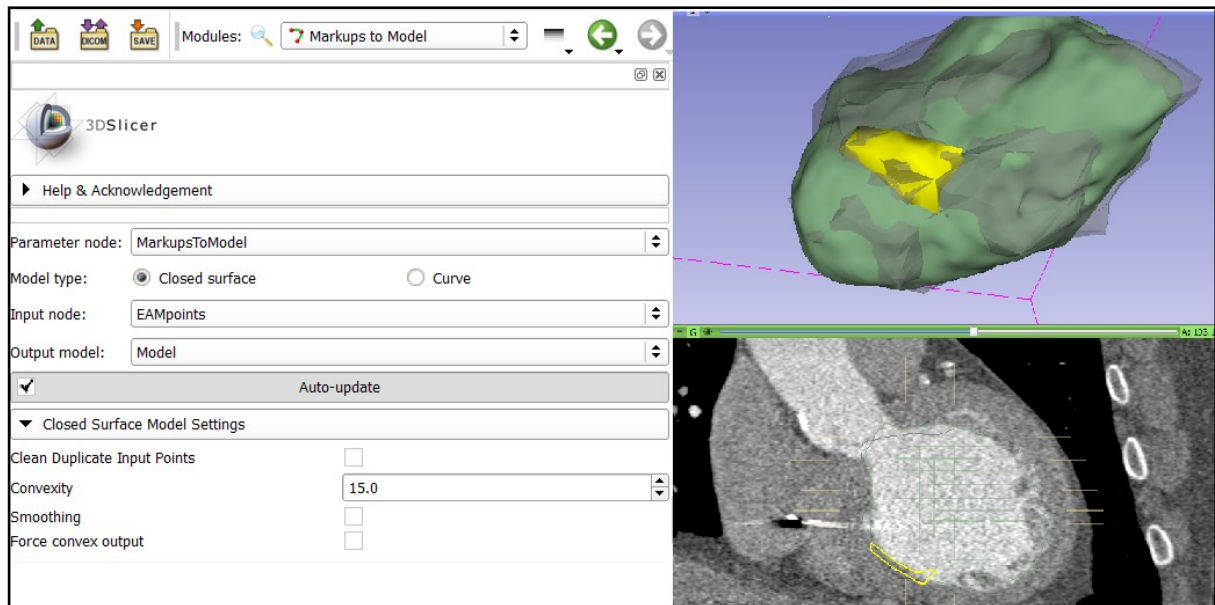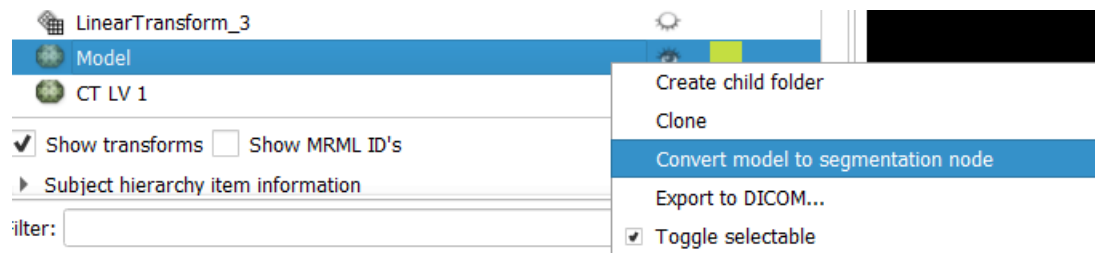

9) Masking the created model onto the CT image series as high-density pixels

The model created in Step 8 is must be converted to segmentation before masking.

9.1.) 3D Slicer version > 4.10

Select the model from step 8 in **Data** module, press the right mouse button, and choose **Convert model to segmentation node.**

9.2.) 3D Slicer version < 4.10

    a. Select the **Segmentations** module from the drop-down menu and **Create new Segmentation** under Active segmentation.

    b. **Representations** tab: set **Make Master** for **Closed Surface**.

    c. **Export/Import models and labelmaps** tab: Operation - **Import**, Input type - **Models**.

    d. Choose the model created in step 8 as **Input node** and do **Import**.
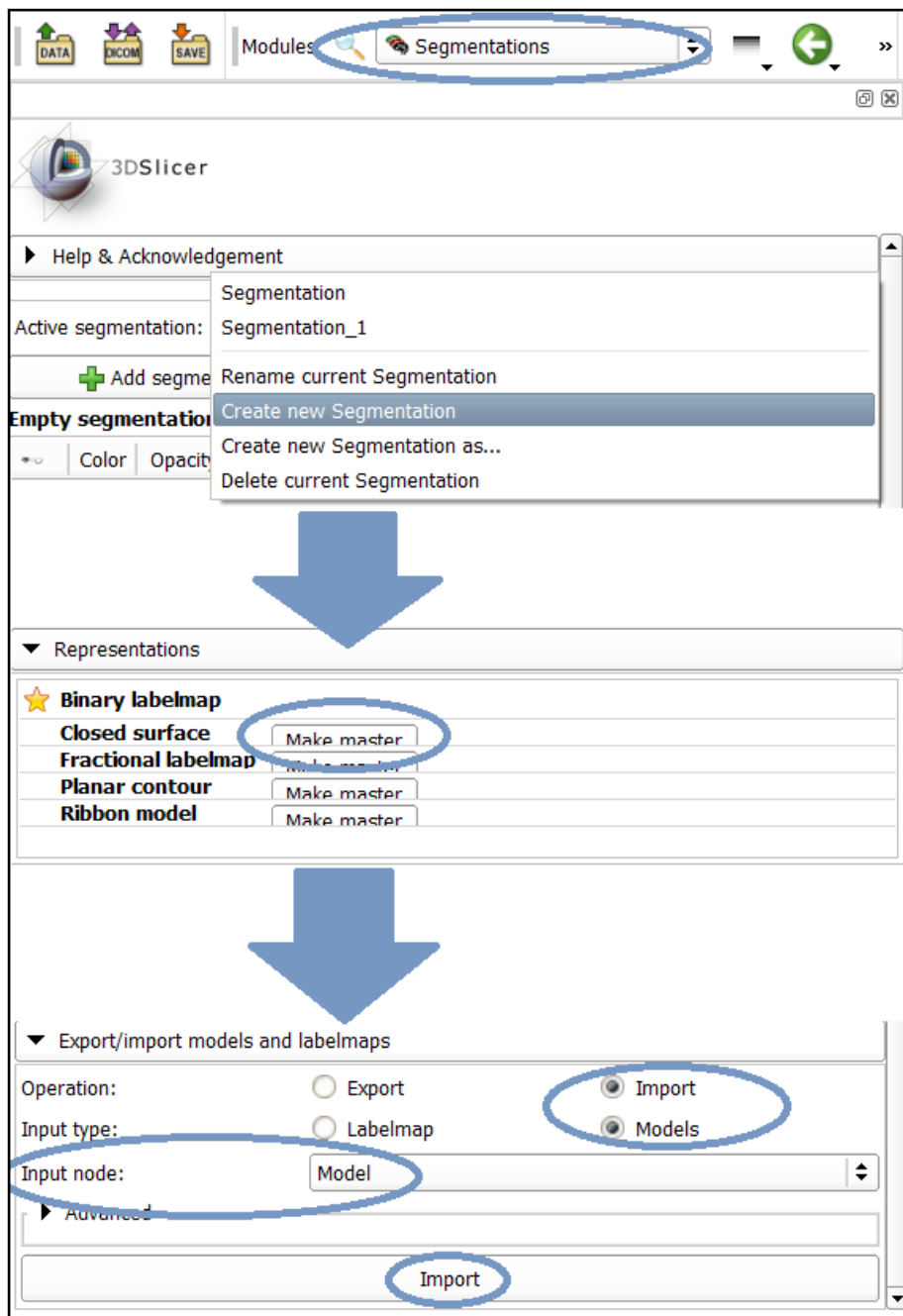
e. After converting the final model of the target, select **Segment editor** from the drop-down menu.

f. As **Segmentation**, choose Segmentation, which contains the target segment.

g. Select your CT data as **Master volume**.

h. **Effects** tab: choose **Mask Volume** (confirm change of representation to binary labelmap).

i. **Mask Volume** tab:

- **Operation**: Fill inside

- **Fill value**: 2000 (number defines the pixel intensity; we prefer high intensity propagating in high HU in CT image).
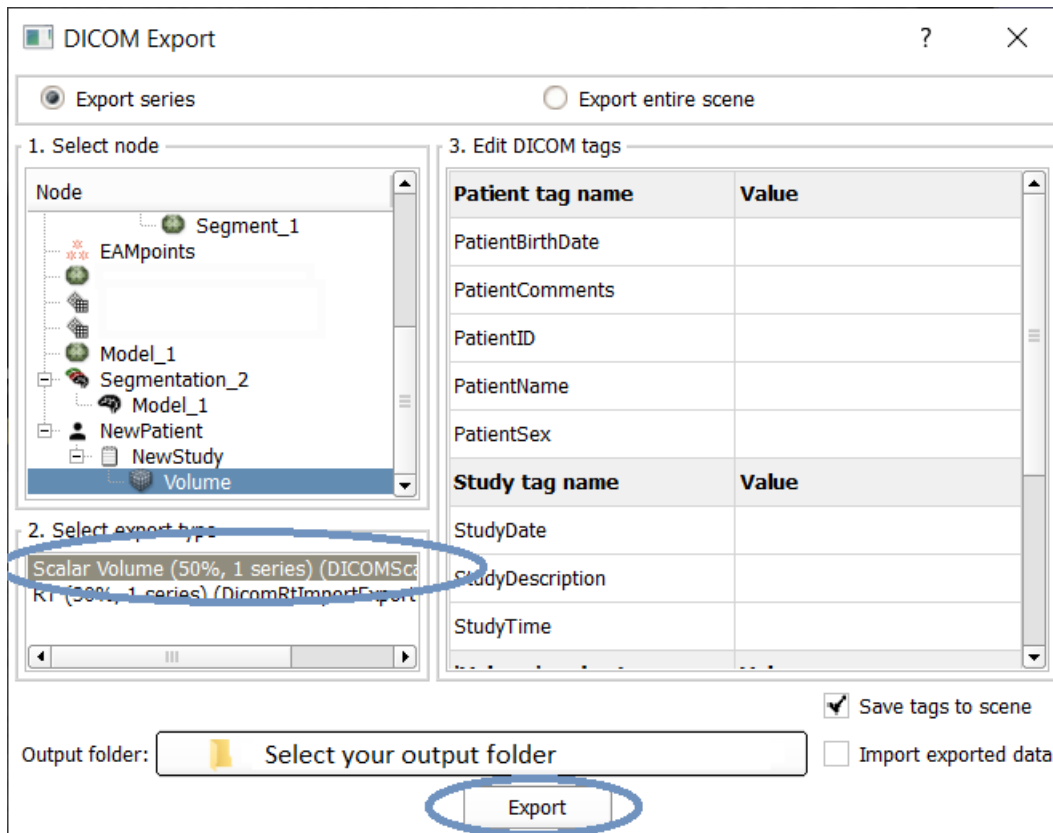- **Output Volume:** create new Volume

j. **Apply**.
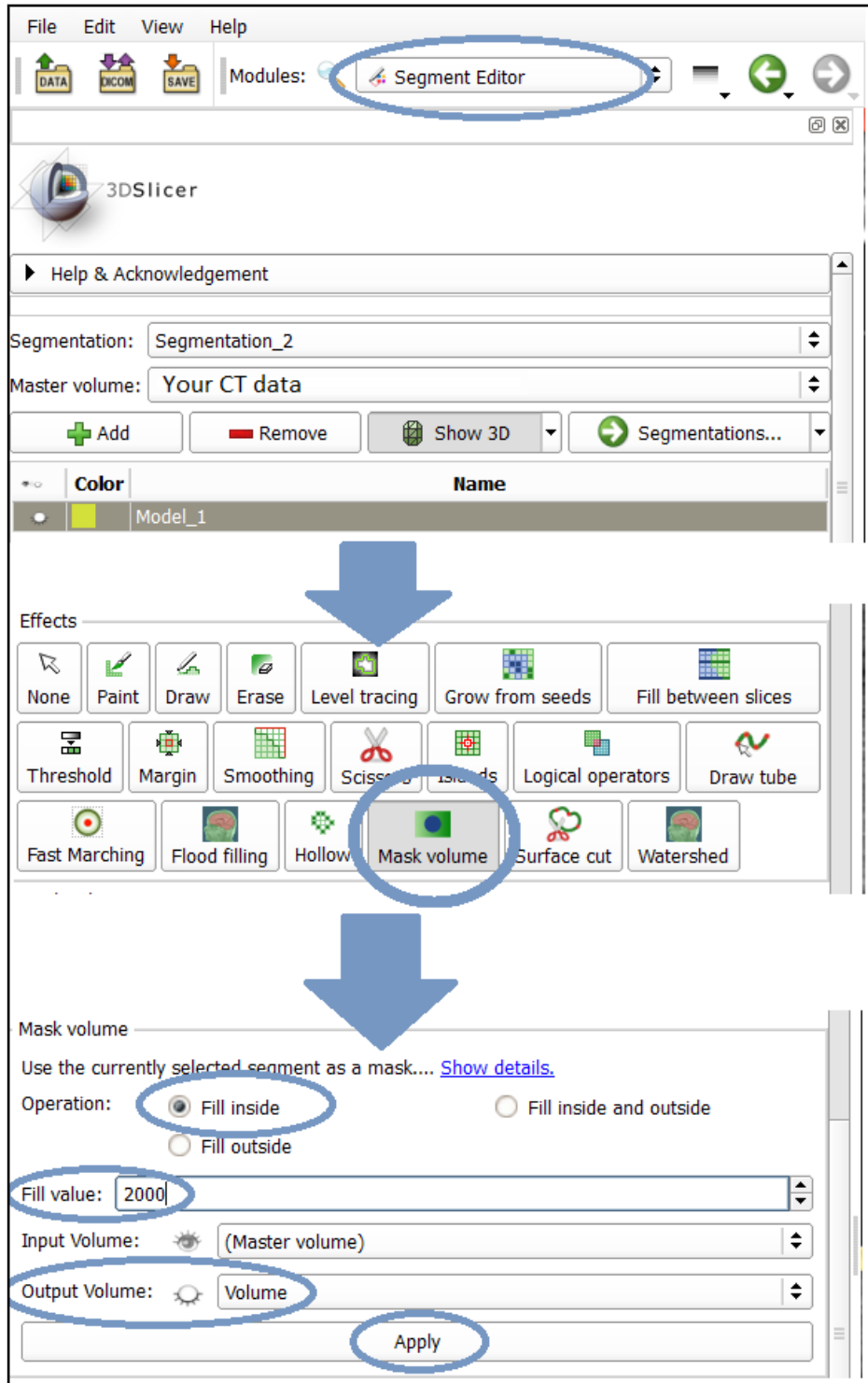
10) Exporting CT from 3D Slicer software and uploading to the planning system

a. Select the **Data** module in the drop-down menu. Your volume with masked structure should be at the bottom.

b. Click the right mouse button and choose **Export to DICOM**.

Note: Import to planning system is based on the software you use. We noted that some systems encounter a problem with "Unknown" Scanner Manufacturer and Scanner Model (this is how 3D Slicer exports). In this case, you need to modify specific DICOM tags before importing (tag 00080070 and 00081090).

Additional information for the smoothing method from step 3:

In 3D modeling, median, opening, and closing filters are types of filters that can be used to smooth or modify the surface of a 3D model.

A median filter in 3D modeling can be used to smooth the surface of a 3D model by replacing the value of each vertex with the median value of the vertices in a surrounding window. This step can be useful for removing noise or small details that are not important for the final model.

An opening filter in 3D modeling can be used to remove small features or separate connected components in a 3D model. This step is achieved by eroding the edges of the

objects in the model and then dilating the model to restore the original size of the objects. Opening filters are often used as a preprocessing step before applying other image processing techniques, such as thresholding or edge detection.

A closing filter in 3D modeling is the opposite of an opening filter. It works by dilating the edges of the objects in the model and then eroding the model to restore the original size of the objects. Closing filters are often used to fill in small holes or gaps in a model, or to smooth out rough edges.

In summary, a median filter is used to smooth the surface of a 3D model, an opening filter is used to remove small features or separate connected components, and a closing filter is used to fill in small holes or smooth out rough edges.

We tested different filters and combinations of parameters in 3D Slicer to maximize the robustness of the proposed method and reproducibility (minimalize intra/interobserver variability), which resulted in use of median 5-mm filter.
Demonstration of the effect of different filtering on the segmentation: